

Neutron-Proton Polarization and Differential Cross Section at 128 Mev*†

RUSSELL K. HOBBIE AND DOUGLAS MILLER
Cyclotron Laboratory, Harvard University, Cambridge, Massachusetts

(Received August 1, 1960)

A 42% polarized neutron beam of 128 Mev average energy has been used to measure the n - p differential cross section and polarization. A range telescope detected recoil protons from a liquid hydrogen target placed in the beam. The following values were obtained:

$\theta_{c.m.}$	σ	P
169.7	11.37 ± 0.41	$+0.002 \pm 0.021$
159.3	9.08 ± 0.33	-0.045 ± 0.021
149.0	7.30 ± 0.26	-0.061 ± 0.021
138.8	6.28 ± 0.23	-0.072 ± 0.017
128.5	5.20 ± 0.19	-0.016 ± 0.021
118.4	4.29 ± 0.15	$+0.054 \pm 0.021$
108.2	3.45 ± 0.12	$+0.052 \pm 0.025$
98.1	2.83 ± 0.11	$+0.186 \pm 0.028$
88.1	2.61 ± 0.09	$+0.275 \pm 0.028$
78.1	2.74 ± 0.11	$+0.384 \pm 0.028$

The errors quoted do not include the 7% uncertainty in the normalization of the cross-section data or the 8% uncertainty in the normalization of the polarization data.

INTRODUCTION

THE polarization parameter for the n - p interaction can be measured either by scattering polarized protons inelastically from deuterons¹⁻³ or by scattering polarized neutrons from protons.⁴⁻⁶ The second method has the advantage of being a two-body process; however, low beam polarizations (8%-16%) have so far limited the accuracy of this method. The 43% polarized neutron beam obtained from the Harvard University synchrocyclotron by scattering neutrons from a carbon polarizer⁷ overcomes this limitation.

This paper describes measurements of the n - p polarization and differential cross section in the range from 80°-170° c.m. Recoil protons from a liquid hydrogen target placed in the polarized neutron beam were detected with a range telescope.

BEAM CHARACTERISTICS

The beam characteristics have been described in the earlier paper,⁷ except as noted below. The volume of the polarizer was increased during the present measurements. The energy spectrum is shown in Fig. 1. With

* Supported by the joint program of the Office of Naval Research and the U. S. Atomic Energy Commission.

† This work is part of a Ph.D. Thesis submitted by R.K.H. to Harvard University.

¹ O. Chamberlain, E. Segre, R. Tripp, C. Wiegand, and T. Ypsilantis, *Phys. Rev.* **105**, 288 (1957).

² A. F. Kuckes and Richard Wilson, *Bull. Am. Phys. Soc.* **4**, 61 (1959); *Phys. Rev.*, (to be published).

³ R. E. Warner and J. H. Tinlot, *Bull. Am. Phys. Soc.* **5**, 282 (1960).

⁴ C. Whitehead, S. Tornabene, and G. H. Stafford, *Proc. Phys. Soc. (London)* **75**, 345 (1960).

⁵ G. H. Stafford, C. Whitehead, and P. Hillman, *Nuovo cimento* **5**, 1589 (1957).

⁶ R. T. Siegel, A. J. Hartzler, and W. A. Love, *Phys. Rev.* **101**, 838 (1956).

⁷ D. Miller and R. K. Hobbie, *Phys. Rev.* **118**, 1391 (1960).

the absorbers in the recoil proton telescope establishing a 110 Mev cut-off energy, the average beam energy was 128 ± 1 Mev, and the rms energy spread was 13 Mev. The flux was 3.7×10^5 neutrons/in.² min through a 2 in. by 6 in. aperture.

The beam polarization was determined from the measured asymmetry of neutrons scattered from a carbon analyzer, as described in the earlier paper. With the increased polarizer volume the polarization was

$$P_b = 0.425 \pm 0.034.$$

APPARATUS AND PROCEDURES

The arrangement of the counters in the recoil proton telescope is shown in Fig. 2. The defining counter C2 was 2 in. wide and 6 in. high. Counter C1 was 2.9 in. by 6.9 in., and C3 was 3.3 in. by 8.1 in. All were made of $\frac{1}{8}$ in. thick Pilot Scintillator B attached by Lucite light pipes to RCA 6810A photomultiplier tubes. The counter spacing shown in Fig. 2 was used for laboratory angles of 20° and greater. For angles of 25° and smaller, the defining counter was placed $65\frac{5}{8}$ inches from the target, with the spacing between the three counters unchanged. The overlap at 20° and 25° provided a check on the normalization of the counting rates when calculating the cross section.

The thickness of the polyethylene absorbers between C2 and C3 was adjusted at each scattering angle to impose a cut-off energy of 110 Mev for neutrons interacting at the center of the target.

A 4 in. by 8 in. by $\frac{1}{8}$ in. anticoincidence counter, A, placed across the beam pipe exit, protected against any proton contamination in the beam. The desired signal was a triple coincidence (C1C2C3) in anticoincidence with the fourfold coincidence (C1C2C3A). This protection was necessary only at a laboratory angle of 5°,

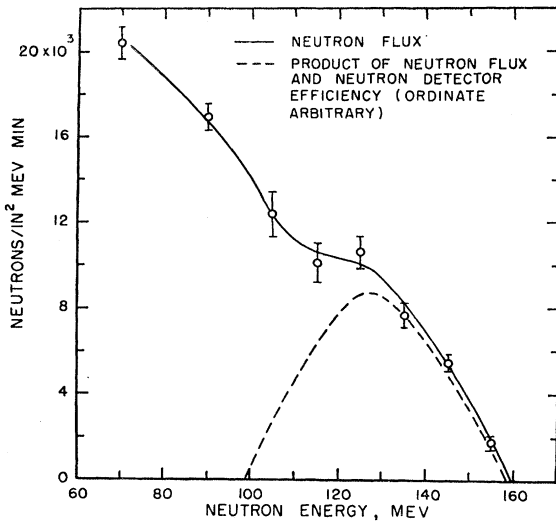


FIG. 1. Energy spectrum of polarized neutron beam. The dashed line shows the product of the neutron flux and the efficiency of the neutron detector used to measure the beam polarization (see reference 7). For the recoil proton measurements a cutoff of 110 Mev was imposed.

where the fourfold rate was about 10% of the threefold rate. At all other angles the fourfold rate was <2%.

The counters were mounted on an arm 11 in. below the median plane. The arm rotated about a pivot located beneath the hydrogen target. The pivot⁸ allowed complete rotational freedom about the vertical axis and limited freedom of rotation in all other directions. This design reduced stress on the pivot when it was not level. The apparatus was levelled by adjusting two support screws at the rear of the arm.

A steel tube which passed through the pivot ball was pressed into an aluminum plate attached to the arm. When the surface of this plate was level, the axis of the tube was vertical. It was then possible, by sighting through the tube and a Lucite window on the bottom of the outer can of the hydrogen target, to align the target with the pivot (Fig. 3).

The scattering angle was determined by the chord from a pin located on the beam axis to a similar pin on the arm. Both pins were 80 in. from the pivot. The beam axis was determined both optically and from the transverse intensity distribution of the beam.⁷ The alignment accuracy was ± 0.03 in.

The liquid hydrogen target was a modification of the design used by Palmieri.⁹ The scatterer was contained in a cylinder of 0.003 in. Mylar, 2 in. diameter by $11\frac{5}{8}$ in. long. This length avoided illumination of any metal portions of the target by the beam. The outer Mylar window was 0.01 in. thick.

Two monitors were used. A recoil proton telescope, viewing a piece of polyethylene located in the beam

⁸ The pivot used an LHA series bearing manufactured by the Heim Company, Fairfield, Connecticut.

⁹ J. N. Palmieri, A. M. Cormack, N. F. Ramsey, and Richard Wilson, *Ann. Phys.* **5**, 299 (1958).

downstream from the hydrogen target, detected neutrons with energies greater than 110 Mev. A BF_3 proportional counter detected low energy neutrons from the cyclotron. The recoil monitor provided a more direct measurement of the beam intensity, but its rate changed by 9% when the hydrogen target was emptied. A correction for this effect was made using the BF_3 monitor.

After alignment of the pivot, target and counter, the target was filled and counter voltages were set on plateaus with the telescope at 20° . Delay curves were checked. Random coincidence rates were measured and found to be negligible.

Proton asymmetries were measured at laboratory angles from 20° to 50° in 5° steps until the target was nearly empty. The target was emptied and evacuated for background measurements. When the backgrounds were completed the alignment of the pivot, target and defining counter was checked optically. The target was refilled and the cycle repeated until the desired statistical accuracy had been obtained. The counter geometry was then changed, and measurements at angles from 5° to 25° were made following the same pattern.

DATA REDUCTION AND CORRECTION

The asymmetry due to scattering from hydrogen is obtained from measurements with the target full and empty:

$$e = \frac{(N^{\text{full}} - N^{\text{empty}}) - (S^{\text{full}} - S^{\text{empty}})}{(N^{\text{full}} - N^{\text{empty}}) + (S^{\text{full}} - S^{\text{empty}})} \quad (1)$$

This is equivalent to the expression

$$e = \left(\frac{r}{r-1} \right) e^{\text{full}} - \left(\frac{1}{r-1} \right) e^{\text{empty}}, \quad (2)$$

where

$$r = (N+S)^{\text{full}} / (N+S)^{\text{empty}}.$$

The values of the two terms in Eq. (2) are plotted in Fig. 4 to show the relative importance of background asymmetries.

The effect of background on the cross-section measurements may be seen in Fig. 5. Rates with the

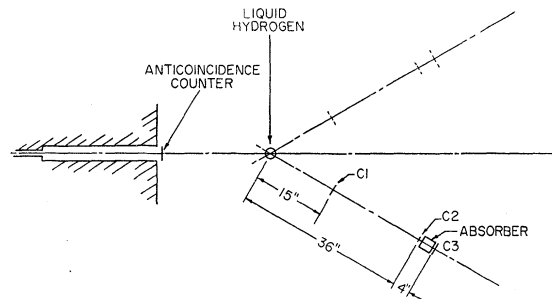


FIG. 2. Counter geometry for detection of recoil protons at laboratory angles of 20° and greater. Changes for small angle measurements are discussed in the text.

TABLE I. Measured and corrected asymmetries. Corrections are given in the form of false asymmetries defined by the equation, $e_{\text{meas}} = e_{\text{true}} + e_{\text{false}}$.

Cause	Large radius					Small radius						
	5°	10°	15°	20°	25°	20°	25°	30°	35°	40°	45°	50°
Alignment of defining counter	0.000 ±0.000	0.000 ±0.001	0.000 ±0.001	0.000 ±0.003	0.000 ±0.003	0.000 ±0.004	0.000 ±0.004	0.000 ±0.005	0.000 ±0.005	0.000 ±0.006	0.000 ±0.006	0.000 ±0.006
Counter and target height	-0.001 ±0.001	-0.001 ±0.001	0.000 ±0.001	0.000 ±0.001	0.000 ±0.001	+0.001 ±0.001	+0.001 ±0.001	+0.001 ±0.001	+0.001 ±0.001	+0.001 ±0.001	+0.001 ±0.001	+0.001 ±0.001
Energy spread	0.000 ±0.000	0.000 ±0.000	0.000 ±0.001	-0.001 ±0.001	-0.001 ±0.001	-0.001 ±0.001	-0.001 ±0.001	-0.001 ±0.001	-0.003 ±0.002	-0.005 ±0.003	-0.006 ±0.003	-0.003 ±0.003
Magnetic field	-0.001 ±0.000	-0.002 ±0.000	-0.003 ±0.001	-0.003 ±0.001	-0.004 ±0.001	-0.002 ±0.000	-0.002 ±0.000	-0.003 ±0.001	-0.003 ±0.001	-0.004 ±0.001	-0.005 ±0.001	-0.005 ±0.001
Total false asymmetry	-0.002 ±0.001	-0.003 ±0.002	-0.003 ±0.002	-0.004 ±0.003	-0.005 ±0.003	-0.002 ±0.004	-0.002 ±0.004	-0.003 ±0.005	-0.005 ±0.005	-0.008 ±0.006	-0.010 ±0.007	-0.007 ±0.008
Raw asymmetry	-0.001 ±0.009	-0.022 ±0.009	-0.029 ±0.009	-0.054 ±0.011	-0.012 ±0.014	-0.014 ±0.008	-0.008 ±0.009	+0.020 ±0.008	+0.017 ±0.010	+0.071 ±0.010	+0.107 ±0.010	+0.155 ±0.009
Corrected asymmetry	+0.001 ±0.009	-0.019 ±0.009	-0.026 ±0.009	-0.050 ±0.011	-0.007 ±0.016	-0.012 ±0.009	-0.006 ±0.010	+0.023 ±0.009	+0.022 ±0.011	+0.079 ±0.012	+0.117 ±0.012	+0.162 ±0.012

counters at large radius have been normalized to the small radius results by multiplying by $R=3.229\pm 0.015$. This factor was computed from the distance between the target and defining counter in the two cases. As a confirmation of this value, the ratio determined from the 20° and 25° counting rates is $R=3.25\pm 0.03$.

Raw and corrected asymmetries are presented in Table I, along with the corrections. The largest error aside from counting statistics reflects possible misalignment of the defining counter. Pivot and target misalignment contribute errors of less than ± 0.002 at all angles. The small correction for counter and target height combines two effects which occur when the scattering is not in the horizontal plane. The scattering angle θ is slightly increased, and the asymmetry is reduced to $P_b P_2 \cos\phi$, where ϕ is the deviation of the scattering plane from horizontal. A correction for the energy spread of the beam was made knowing

the beam spectrum $n(E)$ and the approximate energy dependence of the cross section and polarization. The measured asymmetry is

$$e_m = \frac{\int dE n(E)\sigma(E)P_b(E)P_2(E)}{\int dE n(E)\sigma(E)} = P_b(E_0)P_2(E_0) + e_f,$$

where $\sigma(E)$ is the $n-p$ cross section, P_b is the beam polarization, and P_2 the $n-p$ polarization. If the polarizations are written as

$$P_b(E) = P_b(E_0) + p_b(E),$$

$$P_2(E) = P_2(E_0) + p_2(E),$$

the false asymmetry can be obtained from numerical integration of the expression

$$e_f = \frac{\int dE n(E)\sigma(E)[P_b(E_0)p_2(E) + P_2(E_0)p_b(E) + p_b(E)p_2(E)]}{\int dE n(E)\sigma(E)}.$$

A correction was made for the magnetic field of 11 ± 3 gauss in the region traversed by the recoil proton, which increased the scattering angle on the north and decreased the angle on the south. Another possible uncertainty in the asymmetry is due to the energy loss of background protons traversing the liquid hydrogen. This effect was calculated to contribute an error of less than ± 0.001 at all angles except 45° and 50°, where it was ± 0.002 .

Table II lists the corrections to the cross-section data. The correction for the finite size of the counters and target was made knowing the angular dependence of the cross section. The correction for energy spread was made knowing the approximate energy dependence of the cross section. The loss of energy of background

protons traversing the liquid hydrogen was also considered; the correction was based on backgrounds measured with the target removed and with a different energy threshold in the range telescope. The volume correction reflects the loss of energy which protons experience while escaping from the target. The active volume $V(E)$ of the target varies from zero at energies well below cutoff to full volume at energies well above. The exact shape of $V(E)$ was computed as a function of scattering angle to form the basis for this correction. A proton which has recoiled into the solid angle subtended by the telescope may be scattered out again before it leaves the target. The correction for this effect was calculated from the $p-p$ cross section. A correction has also been made, based on both calculations and measure-

TABLE II. Corrections to the cross section, presented as the ratio $\sigma_{\text{true}}/\sigma_{\text{meas}}$. The raw and corrected laboratory cross sections are also presented, in arbitrary units.

Cause	Large radius						Small radius					
	5°	10°	15°	20°	25°	20°	25°	30°	35°	40°	45°	50°
Counter height	1.010 ±0.010	1.010 ±0.010	1.005 ±0.005	1.004 ±0.004	1.003 ±0.003	1.014 ±0.014	1.010 ±0.010	1.009 ±0.009	1.007 ±0.007	1.005 ±0.005	1.003 ±0.003	1.001 ±0.002
Angular resolution	1.001 ±0.000	1.001 ±0.000	1.000 ±0.000	1.000 ±0.000	1.000 ±0.000	1.000 ±0.000	1.000 ±0.000	0.999 ±0.001	0.999 ±0.001	0.998 ±0.002	0.998 ±0.002	0.998 ±0.002
Energy spread	0.997 ±0.001	0.996 ±0.002	0.995 ±0.002	0.995 ±0.002	0.994 ±0.003	0.995 ±0.002	0.994 ±0.003	0.993 ±0.003	0.994 ±0.003	0.995 ±0.002	0.995 ±0.002	0.995 ±0.002
Background energy loss	1.004 ±0.003	1.004 ±0.003	1.005 ±0.003	1.005 ±0.003	1.005 ±0.003	1.005 ±0.003	1.006 ±0.003	1.007 ±0.004	1.010 ±0.005	1.013 ±0.006	1.021 ±0.010	1.047 ±0.020
Volume correction	0.995 ±0.005	0.994 ±0.005	0.992 ±0.005	0.991 ±0.005	0.990 ±0.005	0.991 ±0.005	0.990 ±0.005	0.986 ±0.005	0.980 ±0.005	0.970 ±0.005	0.960 ±0.005	0.936 ±0.005
Double scattering in target	1.0014 ±0.000	1.002 ±0.000	1.002 ±0.000	1.002 ±0.000	1.002 ±0.000	1.002 ±0.000	1.002 ±0.000	1.003 ±0.000	1.003 ±0.000	1.003 ±0.000	1.004 ±0.000	1.005 ±0.001
Absorber losses	1.126 ±0.010	1.123 ±0.010	1.116 ±0.010	1.105 ±0.010	1.093 ±0.010	1.105 ±0.010	1.093 ±0.010	1.080 ±0.010	1.069 ±0.010	1.055 ±0.010	1.041 ±0.010	1.028 ±0.010
Uncertainty in energy cutoff	1.000 ±0.031	1.000 ±0.031	1.000 ±0.031	1.000 ±0.031	1.000 ±0.031	1.000 ±0.031	1.000 ±0.031	1.000 ±0.031	1.000 ±0.031	1.000 ±0.031	1.000 ±0.031	1.000 ±0.031
Total	1.135 ±0.039	1.131 ±0.039	1.115 ±0.037	1.102 ±0.037	1.086 ±0.036	1.113 ±0.040	1.095 ±0.038	1.077 ±0.037	1.061 ±0.036	1.037 ±0.035	1.020 ±0.035	1.006 ±0.039
Raw laboratory cross section	10.391 ±0.105	8.221 ±0.084	6.558 ±0.066	5.531 ±0.069	4.450 ±0.065	5.487 ±0.042	4.489 ±0.038	3.537 ±0.027	2.714 ±0.024	2.120 ±0.022	1.820 ±0.017	1.755 ±0.016
Corrected laboratory cross section	11.794 ±0.424	9.298 ±0.339	7.312 ±0.260	6.095 ±0.229	4.833 ±0.179	6.107 ±0.224	4.915 ±0.177	3.809 ±0.136	2.880 ±0.102	2.198 ±0.082	1.856 ±0.067	1.766 ±0.071

ment in a proton beam, for the loss of protons by nuclear interactions in the absorber between C2 and C3. The largest source of error is uncertainty in the cut-off energy and hence in the neutron flux illuminating the target. This uncertainty does not exceed ± 1 Mev.

Since the beam intensity is not accurately known, the cross section must be normalized by equating the

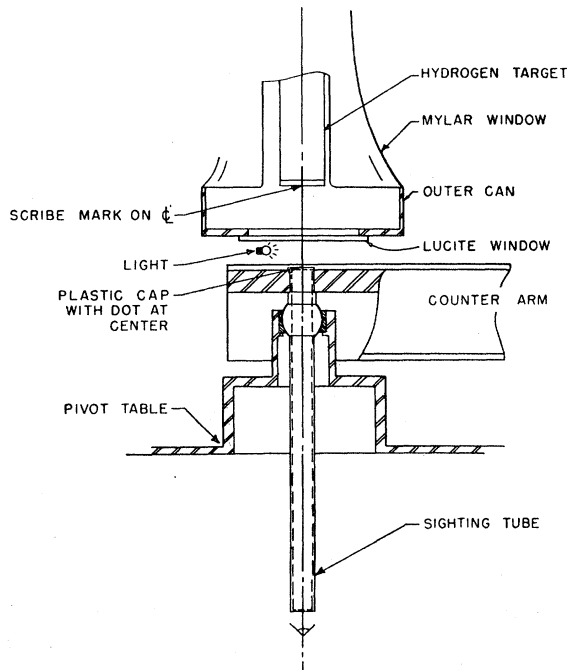


FIG. 3. Cross section of the counter arm, pivot, and hydrogen target, showing how the target was aligned with the pivot.

integral of the cross section to the total cross section, σ_t . This integration cannot be made without knowing the cross section for angles below 80° . Values of the cross section for these angles were obtained by interpolation

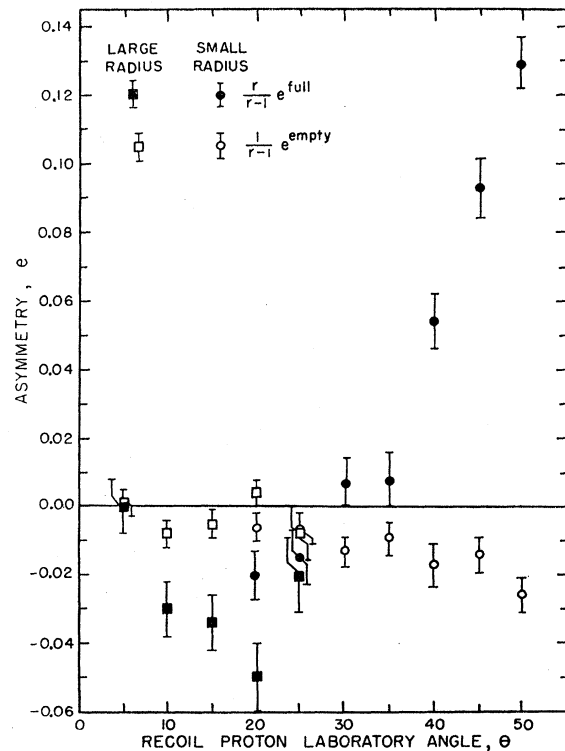


FIG. 4. Recoil proton asymmetries measured with the hydrogen target full and empty, to show the contribution of background asymmetries to the final result.

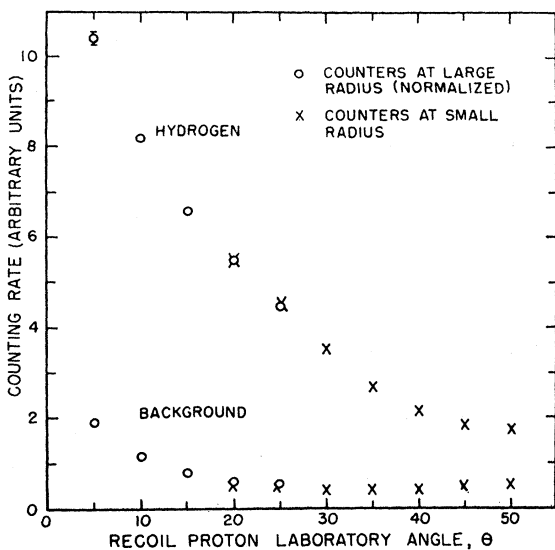


FIG. 5. The $(N+S)$ counting rates for hydrogen scattering and background scattering.

from measurements¹⁰ at 105 Mev and 137 Mev which had been normalized independently of the total cross section by placing the neutron detector in the unscattered beam. The total cross section was taken as $\sigma_t = 56 \pm 2$ mb, an interpolation from the measurements by Taylor and Wood.¹¹ Including the error in the normalization of the small angle data, the error in the normalization of the present work is $\pm 7\%$.

RESULTS AND DISCUSSION

The corrected values of the *n-p* polarization and differential cross section are presented in Table III. The 8% fractional error due to uncertainty in the value

TABLE III. Neutron-proton cross section and polarization results. Errors of $\pm 7\%$ in the normalization of the cross-section data and $\pm 8\%$ in the normalization of the polarization data have not been included.

Recoil proton angle	Center-of-mass scattering angle, θ	$\sigma_{c.m.}$ mb/sr	<i>p</i>
5	169.7	11.37 ± 0.41	$+0.002 \pm 0.021$
10	159.3	9.08 ± 0.33	-0.045 ± 0.021
15	149.0	7.30 ± 0.26	-0.061 ± 0.021
20	138.8	6.28 ± 0.23	-0.072 ± 0.017
25	128.5	5.20 ± 0.19	-0.016 ± 0.021
30	118.4	4.29 ± 0.15	$+0.054 \pm 0.021$
35	108.2	3.45 ± 0.12	$+0.052 \pm 0.025$
40	98.1	2.83 ± 0.11	$+0.186 \pm 0.028$
45	88.1	2.61 ± 0.09	$+0.275 \pm 0.028$
50	78.1	2.74 ± 0.11	$+0.384 \pm 0.028$

¹⁰ J. J. Thresher, R. G. P. Voss, and R. Wilson, Proc. Royal Soc. (London) **A229**, 492 (1955).

¹¹ A. E. Taylor and E. Wood, Phil. Mag. **44**, 95 (1953).

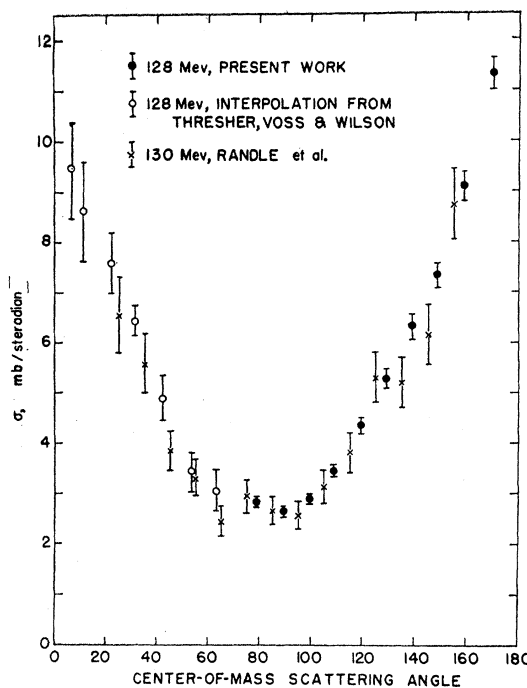


FIG. 6. Neutron-proton differential cross section, showing the present work, the interpolation from the small angle data of Thresher, Voss, and Wilson (reference 10) and the bubble chamber measurements by Randle *et al.* (reference 12).

of the beam polarization has not been included in the tabulated error, since it is a multiplicative error affecting all the polarization results in the same fashion. For the same reason, the 7% normalization error has not been included in the cross-section results.

The cross section is displayed, along with the interpolated small angle data, in Fig. 6. The 130-Mev bubble chamber measurements,¹² which are in good agreement with the present data, are also shown.

The polarization is plotted in Fig. 7 with the 145-Mev inelastic *p-D* measurements by Kuckes and Wilson,² and the 95-Mev measurements by Stafford *et al.*⁵ For the common angles between 80° and 120° the 128-Mev data lie much closer to the 95-Mev points than to those at 145 Mev. Two possible errors which could cause this effect can be excluded. First, the persistence of the effect for angles near 120° where the asymmetry is small indicates that it is not due to an error in measuring the beam polarization. Second, a false asymmetry of this magnitude would require a large misalignment (nearly 1/8 in.). The effect is therefore believed to be real.

The change of polarization with energy may also be demonstrated by plotting the polarization at some angle as a function of energy. This has been done for $\theta = 90^\circ$

¹² T. C. Randle, D. M. Skyrme, M. Snowden, A. E. Taylor, F. Uridge, and E. Wood, Proc. Phys. Soc. (London) **A69**, 760 (1956).

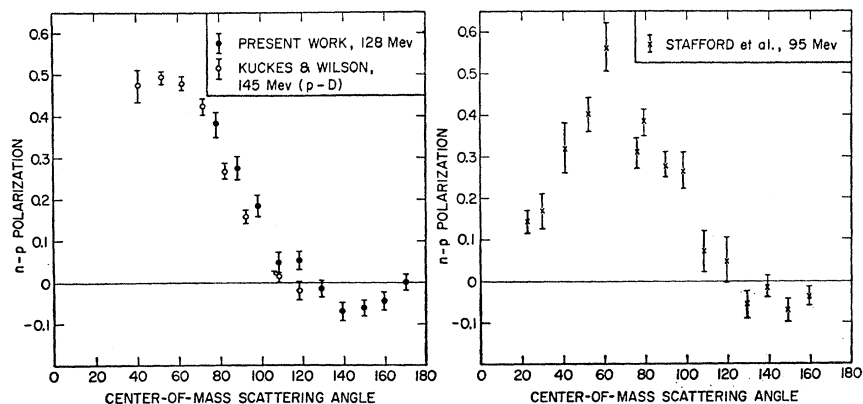


FIG. 7. Neutron-proton polarization. The graph on the left shows the present work with the 145 Mev inelastic p - D results of Kuckes and Wilson (reference 2), while the graph on the right shows the 95 Mev results of Stafford *et al.* (reference 5).

in Fig. 8. The errors on each point have been increased to include errors in the beam polarization measurements. This plot indicates that the fairly abrupt energy dependence takes place above 128 Mev.

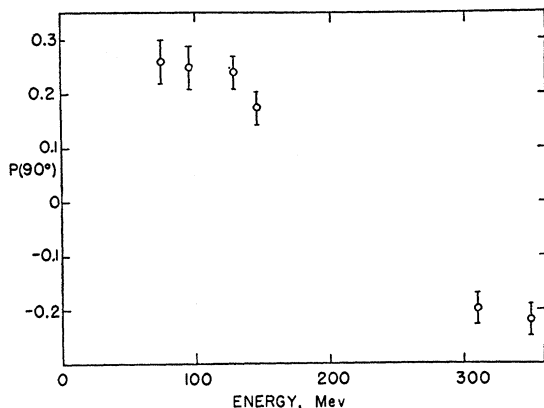


FIG. 8. The n - p polarization at 90° c.m. as a function of energy. In addition to the measurements shown in Fig. 7, values at 77 Mev (reference 4), 310 Mev (reference 1) and 350 Mev (reference 6) have been included.

CONCLUSION

The n - p polarization has been measured at 128 Mev for angles greater than 80° , taking advantage of a high beam polarization to reduce the effect of spurious asymmetries. There are indications of a fairly rapid variation of polarization with energy above 128 Mev. It has also been possible to extract the differential cross section from the data, measuring the shape of the angular distribution to an accuracy of $3\frac{1}{2}\%$.

ACKNOWLEDGMENTS

We are grateful to the entire staff of the cyclotron laboratory for their assistance in making this experiment possible. M. Wanagel and S. Blandino helped design the target and scattering table, while D. Mackie helped to construct the hydrogen target. D. Uhlman, D. Lynch, P. Patel, A. Carroll, and D. Teal, and Miss S. McKee assisted at various times. One of us (R. K. H.) is grateful for the support of a National Science Foundation Cooperative Fellowship.